NUMERICAL MODELING OF PASSING VESSEL IMPACTS ON BERTHED VESSELS AND SHORELINE

Scott Fenical[1], Pavlo Kolomiets[2], Sergey Kivva[2], Mark Zheleznyak[2]

A new numerical model for calculating impacts on berthed vessels and shoreline based on the nonlinear shallow water equations is presented. Comparisons with laboratory and field data, as well as some results of model applications on engineering projects are given.

INTRODUCTION

Surges generated by moving deep-draft vessels contribute to shoreline erosion, re-suspension of sediments in the surf zone, and generate significant hydrodynamic loads on berthed vessels and shoreline structures. It is desired in coastal engineering to limit vessel hydrodynamic impacts on marine resources and aquatic habitat, to improve navigation safety, to minimize risks to berthed vessels from passing vessels, and to minimize potential shoreline erosion. In the present paper, the development and application of the Vessel Hydrodynamics Longwave Unsteady (VH-LU) model and Vessel Hydrodynamics Longwave Load (VH-LL) module are presented. The VH-LU model was developed though cooperation between the Ukrainian Center of Environmental & Water Projects (UCEWP) and Coast & Harbor Engineering (CHE) under a grant from the U.S. Civilian Research & Development Foundation. The VH-LL module was developed by CHE as a complimentary module for use with the VH-LU model. The present paper also presents preliminary verifications of the hydrodynamics model with field data from two projects, and preliminary verification of the hydrodynamics and berthed vessel loading models with laboratory data (Remery 1974).

Existing Modeling Tools and Objectives

Several numerical models exist that are capable of calculating surges from vessels, which are based on different approaches. The most well-known of these modeling approaches are the following:

- Linearized Shallow Water Equations (LSWE): Fenical et al. (2001), MacDonald (2003).
- Nonlinear Shallow Water Equations (NLSWE): Stockstill et al. (1999) implementation of HIVEL2D and ADH numerical finite element codes.

[1] Coast & Harbor Engineering, San Francisco, CA, USA
[2] Ukrainian Center of Environmental and Water Projects, Kiev, Ukraine

- Boussinesq-type Nonlinear Dispersive Shallow Water Equations (BT NDSWE): Nwogu (2003) "Bouss2D," Kofoed-Hansen et al. (2000), "Mike-21 BW."
- Coupling of BT NDSWE and CFD codes: Kofoed-Hansen et al. (2000), "Mike-21 BW" + "SHALLO."

The present numerical model was developed to provide accurate calculations of vessel-induced water level and velocity fluctutions with reasonable computational efficiency, efficient and effective wetting and drying algorithms for simulation of coastal impacts, as well as coupling with sediment transport and coastal erosion modules. To satisfy these requirements, the VH-LU model was developed based on a finite volume code for the NLSWE. The output of the model is also used as input into the VH-LL model to calculate loads on berthed vessels or structures.

VH-LU Governing Equations and Vessel Representation

Water flow is described by the two-dimensional Saint Venant equations with a source term representing the moving vessel. These equations are derived from the general three-dimensional hydrodynamic equations of continuity and motion for an incompressible fluid with a constant density and without consideration of surface tension by vertically averaging the latter over flow depth, and using kinematic boundary conditions. In the derivation of the vertically-averaged equations, the following main assumptions were made for shallow water flow of long-waves: the vertical acceleration of a fluid particle is small in comparison with the acceleration of gravity, the shear stresses due to the vertical velocity component are also small, and the terms due to horizontal shear are small compared with the terms due to vertical shear. The water flow problem representation is shown below in Figure 1.

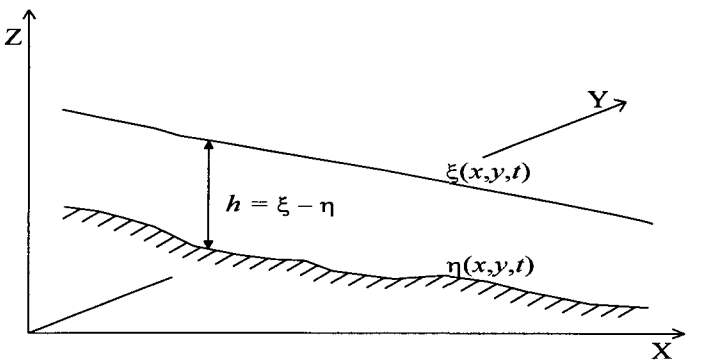

Figure 1. Schematic representation of water flow, Cartesian coordinates.

The model governing equations consist of a continuity equation and two momentum equations. By denoting q_x and q_y (m^2/s) the components of the water discharges per unit width along the horizontal directions x and y, mass conservation yields to

$$\frac{\partial h}{\partial t}+\frac{\partial q_x}{\partial x}+\frac{\partial q_y}{\partial y}=0 \tag{1}$$

where
t is the time variable (s);
x and y are Cartesian coordinates (m);
$\xi(x,y,t)$ is the free surface elevation (m);
$\eta(x,y,t)$ is the bed surface elevation (m);
h is the water depth (m) equals to $\xi-\eta$;

The resulting momentum conservation equations in the x- and y-directions are:

$$\frac{\partial q_x}{\partial t}+\frac{\partial (uq_x)}{\partial x}+\frac{\partial (vq_x)}{\partial y}=-gh\frac{\partial \xi}{\partial x}-\frac{h}{\rho}\cdot\frac{\partial P}{\partial x}+\frac{\partial}{\partial x}\left(D_x\frac{\partial q_x}{\partial x}\right)+\frac{\partial}{\partial y}\left(D_y\frac{\partial q_x}{\partial x}\right)-\frac{1}{\rho}\tau_x^{\eta} \tag{2}$$

$$\frac{\partial q_y}{\partial t}+\frac{\partial (uq_y)}{\partial x}+\frac{\partial (vq_y)}{\partial y}=-gh\frac{\partial \xi}{\partial y}-\frac{h}{\rho}\cdot\frac{\partial P}{\partial y}+\frac{\partial}{\partial x}\left(D_x\frac{\partial q_y}{\partial x}\right)+\frac{\partial}{\partial y}\left(D_y\frac{\partial q_y}{\partial x}\right)-\frac{1}{\rho}\tau_y^{\eta} \tag{3}$$

where
u,v is the x- and y-components of the depth-averaged current velocity (m/s);
ρ is the density of water (kg/m^3);
g is the acceleration of the gravity (m/s^2);
D_x, D_y are the eddy viscosity coefficients in x- and y-directions (m^2/s);
τ_x^{η}, τ_y^{η} are the shear stresses at the bed surface in x- and y-directions ($kg/(m\cdot s^2)$).

The subscripts x and y are the directional index. P is the vessel moving pressure field boundary condition. The pressure field is computed in the same manner as in the model HIVEL2D (Stockstill and Berger, 1999; 2001).

$$P=\rho g\vec{d} \tag{4}$$

where d is the draft of the vessel. For turbulent flow without waves, Reynolds' stress dominates and viscous stress may be negligible. In this case, the bottom shear stress can be approximated by the Manning equation as

$$\tau_x^{\eta}=\rho g\frac{n^2}{h^{1/3}}u\sqrt{u^2+v^2}=c_b u\sqrt{u^2+v^2} \tag{5}$$

$$\tau_y^\eta = \rho g \frac{n^2}{h^{1/3}} v\sqrt{u^2+v^2} = c_b v\sqrt{u^2+v^2} \tag{6}$$

$$c_b = \rho g \frac{n^2}{h^{1/3}} \tag{7}$$

where n is the Manning roughness coefficient ($s/m^{1/3}$).

If waves do not contribute significantly to mixing, the eddy viscosity coefficient D depends on the total water depth, current speed, and bottom roughness (Falconer, 1980) and can be calculated by the formula:

$$D_0 = \frac{\theta}{2}\left[1.156hc_b\sqrt{u^2+v^2}\right] \tag{8}$$

where θ is the weighting parameter.

Loads on Berthed Vessels

The Vessel Hydrodynamics Longwave Load (VH-LL) module calculates loads on structures or vessels based on the hydrodynamic output from the VH-LU model. The model calculates loads on berthed vessels using a plan hull form that is discretized into a set of small linear segments, each with a certain length and orientation. Hydrodynamic data time histories are then utilized to compute static pressures on each segment of hull, with pressure forces all acting normal to the hull, which were summed up to determine the composite forces Fx, Fy and the composite moment based on the location of the center and orientation of each hull segment.

NUMERICAL METHOD

The governing equations are solved by an explicit finite-difference scheme with flux correction (Boris & Book, 1973). The scheme has 1st order temporal and 1st or 2nd order spatial. It is split-directional and has a non-uniform un-staggered rectangular grid. The numerical scheme was tested against a set of the tests used for verification of the M2D model (Militello et al. 2004). Verification tests relevant for vessel hydrodynamics include the long-wave runup and slosh tests.

The flow domain is spatially discretized into a computational domain composed of a number of non-overlapping control volumes. Each control volume surrounds a single grid point, which defines the position of intrinsic property variables. Surfaces between nodes are located at the midpoint between two adjacent nodes. Control volumes are defined by their bounding surfaces (see Fig. 2). Positive and negative directions along the x-axis are referred to as *east* and *west*, respectively. Similarly, positive and negative directions along the y-axis are referred to as *north* and *south*, respectively. The z-axis is assumed

aligned with negative gravitational vector, where positive and negative directions are referred to as *top* and *bottom*, respectively.

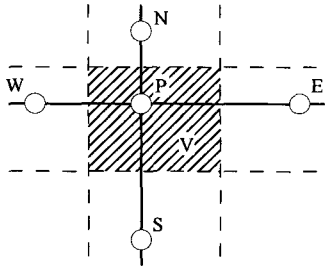

Figure 2. Geometric data for X-Y Cartesian coordinate system.

The calculation domain can be constrained to only the domain surrounding the moving vessel (moving boundary option), thus significantly speeding up the overall simulation. In this case the assumption is made that all the variables at boundaries of such domain are equal to those in the nearest nodes inside the domain.

Momentum Equations

Two momentum equations are solved first using the split-directional finite-volume approximation method. Here, only the x-direction step will be described. The y-direction step is analogous. After computing components of the flow rate at the new time step, new velocity components are calculated which are used by the following continuity equation solver.

X-Direction Step for Momentum Equations

The discretized form of the x-momentum equation for the x-direction step has been written as:

$$\frac{q^{k+1}_{x_{i,j}} - q^{k}_{x_{i,j}}}{\Delta t}\Delta x_{i,j} + \left(F^{k}_{x_{i+0.5,j}} - F^{k}_{x_{i-0.5,j}}\right) + gh^{k}_{i,j}\left(\left(h^{k}_{i+0.5,j} + \eta^{k}_{i+0.5,j}\right) - \left(h^{k}_{i-0.5,j} + \eta^{k}_{i-0.5,j}\right)\right) = \quad (9)$$

$$\left(D^{k}_{x_{i+0.5,j}}\frac{q^{k}_{x_{i+1,j}} - q^{k}_{x_{i,j}}}{x_{i+1,j} - x_{i,j}} - D^{k}_{x_{i-0.5,j}}\frac{q^{k}_{x_{i,j}} - q^{k}_{x_{i-1,j}}}{x_{i,j} - x_{i-1,j}}\right)$$

The discretized form of the y-momentum equation for the x-direction step is written in form

$$\frac{q^{k+1}_{y_{i,j}} - q^{k}_{y_{i,j}}}{\Delta t}\Delta x_{i,j} + \left(G^{k}_{x_{i+0.5,j}} - G^{k}_{x_{i-0.5,j}}\right) = \left(D^{k}_{x_{i+0.5,j}}\frac{q^{k}_{y_{i+1,j}} - q^{k}_{y_{i,j}}}{x_{i+1,j} - x_{i,j}} - D^{k}_{x_{i-0.5,j}}\frac{q^{k}_{y_{i,j}} - q^{k}_{y_{i-1,j}}}{x_{i,j} - x_{i-1,j}}\right) \quad (10)$$

where
k is the time step;
i,j are the cell location indexes;

Δt is the time step;
$\Delta x_{i,j}$ is the cell length in the x-direction.

Fluxes are calculated with a flux correction algorithm on the basis of a simple 1st order upwind scheme and 2nd order centered scheme (Boris & Book, 1973).

$$F^k_{x_{i+0.5,j}} = F^k_{low x_{i+0.5,j}} + C^k_{x_{i+0.5,j}}\left(F^k_{high x_{i+0.5,j}} - F^k_{low x_{i+0.5,j}}\right)$$

$$F^k_{low x_{i+0.5,j}} = \begin{cases} u_{i+0.5,j} q_{x_{i,j}} & if\ u_{i+0.5,j} > 0 \\ u_{i+0.5,j} q_{x_{i+1,j}} & if\ u_{i+0.5,j} < 0 \end{cases} \tag{11}$$

$$u_{i+0.5,j} = 0.5\left(u_{i,j} + u_{i+1,j}\right)$$

$$F^k_{high x_{i+0.5,j}} = 0.5\left(u_{i,j} q_{x_{i,j}} + u_{i+1,j} q_{x_{i+1,j}}\right)$$

After applying low-order fluxes, the difference between high-order and low-order fluxes is corrected based on the intermediate results $\tilde{q}_x, \tilde{q}_y$.

$$C^k_{x_{i+0.5,j}} = \frac{ss \cdot \max\left[0, \min\left(\left|AF^k_{x_{i+0.5,j}}\right|, ss \cdot \left(\tilde{q}_{x_{i+2,j}} - \tilde{q}_{x_{i+1,j}}\right)\Delta x_{i+1,j} / \Delta t, ss \cdot \left(\tilde{q}_{x_{i,j}} - \tilde{q}_{x_{i-1,j}}\right)\Delta x_{i,j} / \Delta t\right)\right]}{AF^k_{x_{i+0.5,j}}}$$

$$AF^k_{x_{i+0.5,j}} = F^k_{high x_{i+0.5,j}} - F^k_{low x_{i+0.5,j}} \tag{12}$$

$$ss = \mathrm{sgn}\left(AF^k_{x_{i+0.5,j}}\right)$$

$G^k_{x_{i+0.5,j}}$ fluxes are calculated correspondingly, id.est. q_y are substituted instead of q_x. After calculating advection terms, the potential and diffusion terms are applied, where

$$\begin{aligned} D^k_{x_{i+0.5,j}} &= 0.5\left(D^k_{x_{i,j}} + D^k_{x_{i+1,j}}\right) \\ h^k_{i+0.5,j} &= 0.5(h^k_{i,j} + h^k_{i+1,j}) \\ \eta^k_{i+0.5,j} &= 0.5(\eta^k_{i,j} + \eta^k_{i+1,j}) \end{aligned} \tag{13}$$

Source Step for Momentum Equations

Next the source step is performed. The semi-implicit scheme for bottom-stress coefficients is used:

$$\frac{q_{x_{i,j}}^{k+1} - q_{x_{i,j}}^{k}}{\Delta t} = -g(C_b)_{i,j}^{k} \frac{q_{x_{i,j}}^{k+1}}{\left(h_{i,j}^{k}\right)^2} \sqrt{(q_{x_{i,j}}^{k})^2 + (q_{y_{i,j}}^{k})^2} \tag{14}$$

$$\frac{q_{y_{i,j}}^{k+1} - q_{y_{i,j}}^{k}}{\Delta t} = -g(C_b)_{i,j}^{k} \frac{q_{y_{i,j}}^{k+1}}{\left(h_{i,j}^{k}\right)^2} \sqrt{(q_{x_{i,j}}^{k})^2 + (q_{y_{i,j}}^{k})^2}$$

Continuity Equation

As for the momentum equations, the split-directional flux-correction based algorithm is used for solving the continuity equation. The x-direction step is given by:

$$\frac{h_{i,j}^{k+1} - h_{i,j}^{k}}{\Delta t} \Delta x_{i,j} + \left(H_{x_{i+0.5,j}}^{k} - H_{x_{i-0.5,j}}^{k}\right) = 0 \tag{15}$$

where fluxes $H_{x_{i+0.5,j}}^{k}$ are calculated correspondingly to those for the advective terms of momentum equations.

Courant Number

During the entire simulation the time step is being changed to satisfy the Courant condition. As the system of governing equations is nonlinear, the Courant number must include all possible movements of liquid disturbances. The largest velocities are tidal velocities which are given by $u = \sqrt{gh}$. For stability the Courant number is typically less than *0.5*.

Filtering

The moving vessel introduces high-frequency ripples which are not of interest for analysis of longwave surges; therefore, a filter is applied to the water surface throughout the domain at each time step. Figure 3 shows the filter mask.

1	2	1
2	5	2
1	2	1

Figure 3. Filter coefficients mask.

The filter smoothes the water surface elevation so that small waves are filtered out, while relatively long waves (L>10Δx) remain almost unmodified (reducing factor>0.9). Figure 4 shows the reducing factors of the filter for one single filtration. It's clear that the filter acts similarly with different wave

directions, and that for vessel-generated surges (long-waves), the reduction factor is nearly 1.0, meaning the filter has a negligible effect on the longwave results.

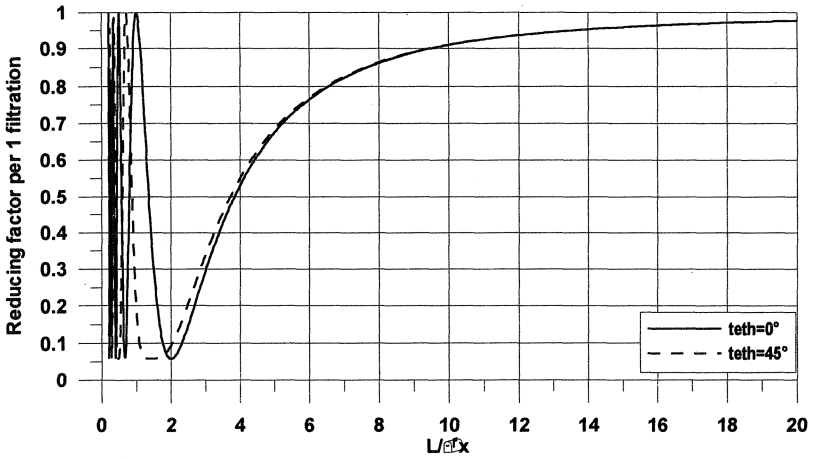

Figure 4. Reducing factor of the filter for wave spreading along axis (solid) and at 45° to axis (dash), Δx=Δy.

Figures 5 and 6 show example filtering results for a simple test with a flat bottom and a vessel moving with constant speed.

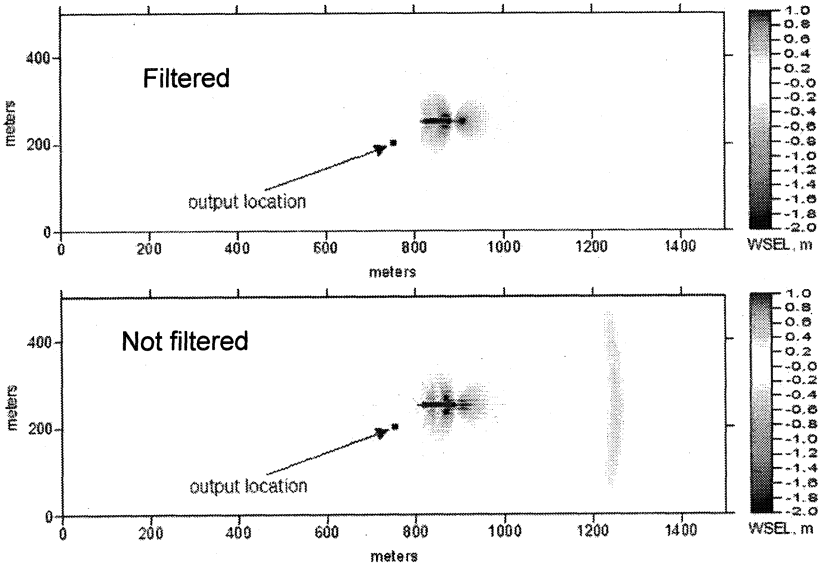

Figure 5. Water surface elevations fields.

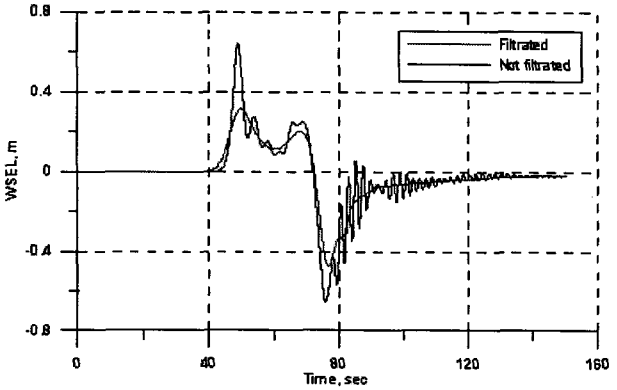

Figure 6. Water surface elevations at output location.

Vessel Routes

The vessel route is developed as a set of small linear segments. Since most vessels of interest have relatively steep sides, the relatively large time step afforded by the model can cause sudden false pressure changes in some nodes during sharp turns. To avoid this, automatic constraints can be set on the maximum vessel rotation and the maximum vessel advancement along the route during each time step. The computational time step is chosen automatically in order to avoid exceeding these limitations, and thereby avoid pressure spikes.

Vessel Hull Specification

The vessel hull is specified using an independent grid whose resolution does not affect the overall simulation speed. This allows us to specify the vessel hull using very fine grids, which results in a better description of moving vessel effects. Vessel hull shapes are input as two-dimensional grids; therefore, 3D features such as bulbous bow features are not included in the model. Hull shapes effectively tested include tankers, containerships, bulk carriers, tug boats and barges.

MODEL FEATURE SUMMARY

The following is a summary of the VH-LU model features:

- Bottom irregularities (input finite-difference or rectilinear grids)
- Variable bottom roughness
- Ambient water level and current fluctuations (boundary as well as initial conditions) due to tides, winds and waves (including linear wavemakers)
- Vessel hull shapes (independent finite-difference grid)
- Variable ship acceleration, speed, and arbitrary sailing line within domain
- Wetting and drying, overland flooding

- Moving calculation boundaries, allowing efficient computation of effects near the vessel over unlimited domains
- Optional calculation of sediment transport, erosion and deposition of variable sized cohesive or non-cohesive sediments over the entire domain
- Multiple output formats, making the model compatible with multiple GUIs

PRELIMINARY MODEL VERIFICATION

The VH-LU model has been verified using water surface elevation and velocity measurements from the Port of Oakland, CA and the Mississippi River Gulf Outlet (MRGO), LA. In addition, the VH-LU hydrodynamics model and VH-LL berthed vessel load calculation system has been verified using laboratory data of Remery (1974). The following is a brief description of the verification; the full verification is under preparation and will be presented in Fenical (2007). Figure 7 shows comparisons of water level fluctuations in the Port of Oakland Inner Harbor Waterway in May 1999 for four different containerships. The predicted and measured water levels show strong correlation. Differences between measured and predicted water levels are likely due to errors in vessel positioning and speed (both determined from RADAR data) and uncertainties in the loading conditions of the passing vessels.

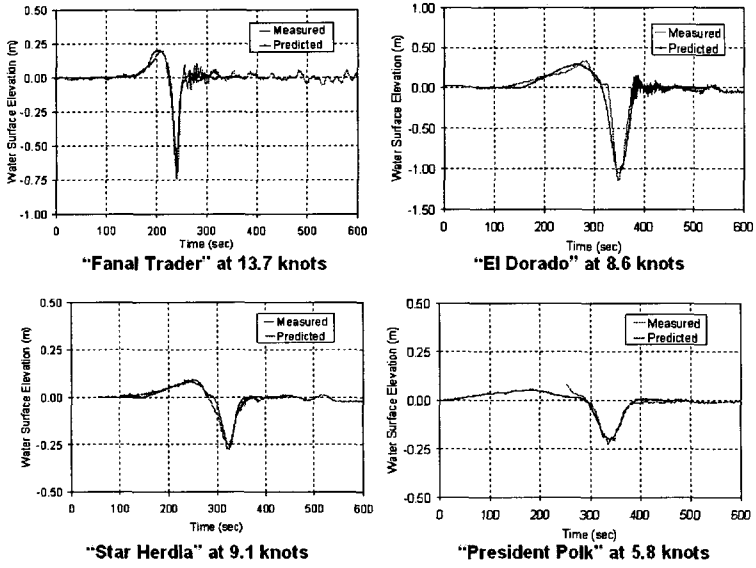

Figure 7. Water surface elevation comparisons in Inner Harbor Waterway, Port of Oakland, May 1999.

Figure 8 shows the water level fluctuations (left) and velocity fluctuations (right) in the MRGO in June 2002 generated by the "TMM Tabasco". Figure 9 shows a preliminary comparison of these results with water level fluctuations (left) and velocity fluctuations (right) measured in the MRGO by the U.S. Army Corps of Engineers, New Orleans District. The predicted and measured water levels and velocities show a strong correlation.

The VH-LU model and VH-LL load calculation module were verified using the Remery (1974) laboratory data set from the Netherlands Ship Model Basin. The study consisted of laboratory measurements of loads on berthed vessels due to passing vessels at a scale of 60:1. Figure 10 shows comparisons of measured and predicted a) longitudinal force, b) lateral force, and c) moment on the 100-MDWT berthed vessel during passing of a 160-MDWT vessel at 7 knots with 30-meter passing distance. In Figure 9 the dashed line is the Remery average time history from multiple runs, the solid line is VH-LU model results, and the dots are individual Remery run data.

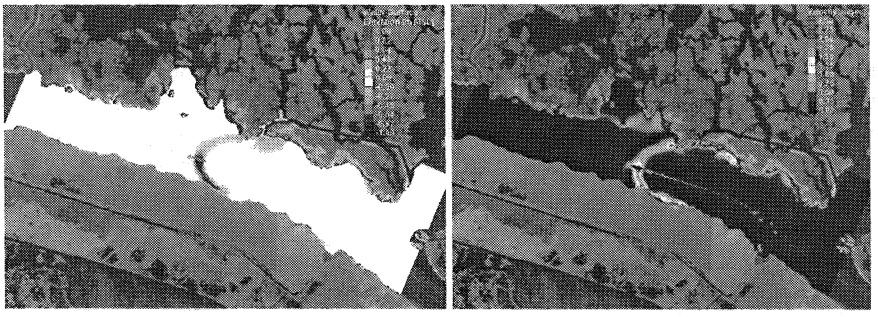

Figure 8. Computed water surface elevation (left) and velocity (right) in the Mississippi River Gulf Outlet (MRGO) during passing of TMM Tabasco, June 2002.

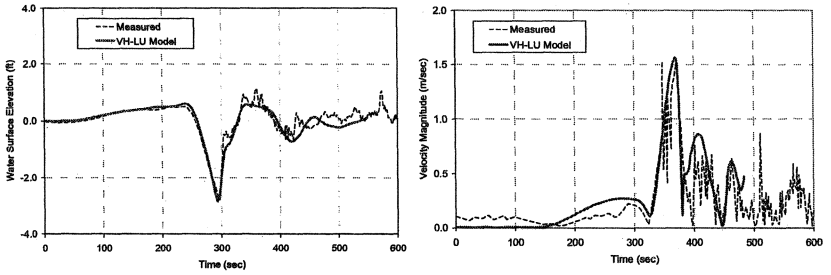

Figure 9. Water surface elevation (left) and velocity (right) measured and computed in the Mississippi River Gulf Outlet (MRGO) during passing of TMM Tabasco, June 2002.

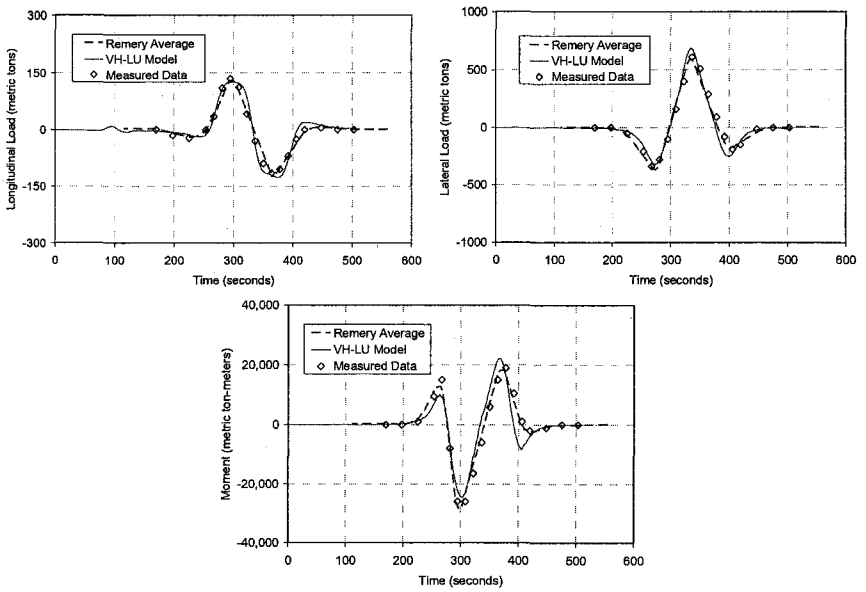

Figure 10. Verification of VH-LU and VH-LL modeling system for measured loads on berthed vessel from Remery (1974).

CONCLUSIONS

The VH-LU and VH-LL numerical models were developed to assist in engineering evaluations of the impacts of passing deep-draft vessels on the shoreline, aquatic resources, and berthed vessels or structures. The numerical models show accurate representation of the hydrodynamic processes for deep-draft vessels, and compute these processes in a highly efficient manner suitable for engineering use on a wide range of navigation projects. Ongoing development of the vessel hydrodynamic modeling system will include refinement of vessel-induced morphology simulations, additional verification with field and laboratory data, inclusion of dispersive Boussinesq equations, and inclusion of a coupling module to enable automatic coupling with RANS-type CFD codes for simulation of wakes generated by high-speed craft.

REFERENCES

Boris, J.P. and Book, D.L. 1973. Flux corrected transport, 1 SHASTA, a fluid transport algorithm that works, *J. Comp. Phys.*, 11, 38-69.

Falconer, R.A. 1980. Modelling of planform influence on circulation in harbors, *Proceedings of the 17th Coastal Engineering Conference*, American Society of Civil Engineers, ASCE Press, New York, 2,726-2,744.

Fenical, S., MacDonald, N. and Yang, F. 2001. "Vessel Hydrodynamic Investigations," Prevention First Symposium, 2001.

Fenical, S. 2007. "Vessel Hydrodynamics and Berthed Vessel Loading Model Verification with Field Data and Laboratory Data," Ports 2007.

Kofoed-Hansen, H., Jensen, T., Kirkegaard, J. and Fuchs, J. 1999. "Prediction of wake wash from high-speed craft in coastal areas." Proc. Conf. Hydrodynamics of High Speed Craft, pp. 24-25.

MacDonald, N. 2003. "Numerical Modeling of Coupled Drawdown and Wake," Canadian Coastal Conference, 2003.

Militello, A., Reed, C., Zundel, A. and N. Kraus. 2005. "Two-Dimensional Depth-Averaged Circulation Model M2D: Version 2.0, Report 1, Technical Documentation and User's Guide." ERDC/CHL TR-04-02.

Nwogu, O. 2001. "Bouss2D: A Boussinesq Wave Model for Coastal Regions and Harbors," ERDC/CHL TR-01-25.

Remery, G.F.M. 1974. "Mooring Forces Induced by Passing Ships," Offshore Technology Conference, Paper Number OTC 2066.

Shepsis, V., Fenical, S., Hawkins-Bowman, B., Dohm, E. and F. Yang. 2001. "Deep-Draft Vessels in Narrow Waterway – Port of Oakland 50-foot Deepening Project." Ports 2001.

Stockstill, R.L. and Berger, R.C. 1999. "A two-dimensional flow model for vessel-generated currents." Prepared for U.S. Army Engineer District, Rock Island, U.S. Army Engineer District, St. Louis, U.S. Army Engineer District, St. Paul, 167 pp., ENV report 10.

Stockstill, R.L. and Berger, R.C. 2001. "Simulating barge drawdown and currents in channel and backwater areas." J. Waterway, Port, Coastal and Ocean Engineering, 127, No. 5, 290-298.